Morris, N., Forder, M., Dolatabadi, N., King, P., Rahmani, R., Rahnejat, H. and Howell-Smith, S., "Oil control ring friction and low viscosity lubricants: A combined numerical and experimental analysis", Proc. Lubrication, Maintenance and Tribotechnology (LUBMAT 2023), 17-19th July 2023, Preston, UK, 9 pp.

Oil Control Ring Friction And Low Viscosity Lubricants: A Combined Numerical and Experimental Analysis

N. Morris[1], M. Forder[1], N. Dolatabadi[1], .P King[1], R. Rahmani[1], H. Rahnejat[1,2] and S. Howell-Smith[3]

[1]Wolfson School of Mechanical, Electrical and Manufacturing Engineering, Loughborough University, Loughborough, UK

[2]School of Engineering, University of Central Lancashire, Preston, UK

[3]Capricorn Automotive Ltd., Basingstoke, UK

Keywords: IC engines; Lubrication; Oil Control Ring

Abstract

A common strategy to reduce engine parasitic power losses is to decrease pumping and viscous friction losses through use of a low viscosity engine oil. However, reducing lubricant viscosity can also decrease the contact load carrying capacity, thus exacerbating direct interaction of contacting surfaces. This leads to boundary frictional losses in contacts prone to mixed regime lubrication. As a result, detailed experimental and modelling studies of engine component frictional behaviour is required to ensure the engine level trade-offs. This paper presents a combined experimental and numerical investigation of frictional behaviour of three-piece piston oil control rings.

A bespoke tribometer replicates kinematics of the contact between a full oil control ring and the cylinder liner. The three-piece oil control ring is composed of two segments, separated by a waveform type expander. The experimental results indicate the dominance of mixed regime of lubrication throughout the stroke. This is particularly the case when the experiments are conducted at 80 °C; a typical engine sump temperature, when compared with the case of 20 °C (a typical engine start-up temperature in the UK in the Spring).

A mixed hydrodynamic numerical model of the oil control ring-cylinder liner tribological interface is employed to apportion frictional contributions with their physical underlying mechanisms. The combined experimental-predictive approach provides key information for engine designers when considering the efficiency trade-offs.

Introduction

The oil control ring spreads the crank-case lubricant supply to the upper scraper ring and the piston compression rings. The oil control ring design effects the lubricant blow-by to the combustion chamber and can potentially cause starvation of compression and scrapper

rings. In addition it also contributes significantly to piston-cylinder parasitic losses. There are several common oil control ring designs. One of the most common type is the three-piece oil control ring, which is investigated in the current study.

Three-piece oil control rings comprise 3 constituent parts; a top and a bottom segment separated by an expander. The outermost radial surface of the segments form lubricated contact conjunctions with the cylinder wall. The expander axially separates the other segments and provides radial tension through the segment seats. A number of studies have been conducted to investigate the losses of various oil control ring types. Two-piece oil control rings have been investigated by Profito et al [1], Söderfjäll et al [2,3], Liu et al [4], Westerfeld et al [5] and Kikuhara et al [6]. Profito et al [1] used a numerical tribological model to show increased hydrodynamic load carrying support was attained after the cylinder liners were run-in for an extended period of time. Söderfjäll et al [2] employed a tribodynamic model to investigate twin-land oil control rings for use in heavy duty diesel engines. The model was shown to have the capability to quantify ring design changes. In a subsequent paper Söderfjäll et al [3] showed a new test rig for measuring piston ring friction. The results showed that the twin-land oil control ring caused starvation of the upper piston rings. Liu et al [4] used a combined numerical and experimental floating liner test set up to investigate the effect of cross-hatched liners and a twin-land oil control ring upon generated friction. Westerfeld et al [5] used an engine furnished with a floating liner to investigate the effect of various twin-land ring designs and the differences in their frictional behaviour between two and three piece oil control rings. The authors noted that higher sliding speeds were required for the three-piece oil control rings to transition to full hydrodynamic lubrication than the equivalent two-piece oil control rings. Kikuhara et al [6] showed that surface texturing of the cylinder bore/ liner surface could, under some operating conditions reduce viscous frictional losses.

Three-piece oil control rings have also been investigated by Tian et al [7], Zhang et al [8], Li and Tian [9] and Mochizuki et al [10]. Tian et al [7] conducted a tribodynamic study of three-piece oil control ring noting that there is asperity frictional loss across a wide range of engine speeds. Zhang et al [8] conducted a combined experimental and numerical study, employing an optical access engine to investigate oil transportation with a three-piece oil control ring. Li and Tian [9] used the same optical engine with 2D Laser-induced fluorescence to investigate lubricant oil consumption. The study focused on oil accumulation in the ring gaps. Mochizuk et al [10] also investigated lubricant oil consumption and the three-piece oil control ring behaviour, focusing on the role of lubricant inertia, ring dynamics and gas pressure.

A significant body of research has been conducted to investigate various types of oil control rings' performance. The current study presents a combined experimental and numerical predictive approach to fundamentally highlight oil control ring- cylinder liner conjunction.

Methodology

Experimental Piston Ring Facility

A bespoke piston ring tribometer, housed at Loughborough University, is used in the current study to measure oil control ring-cylinder liner friction [11]. The test rig introduces a relative motion between the piston and cylinder bore surface. However, unlike a typical engine, the test rig reciprocates the liner against a spatially fixed ring. This enables the ring to be easily instrumented. Figure 1 shows the experimental set up. The liner is driven by an electric motor (1) via a belt drive (2) connected to a scotch yoke mechanism (3). This arrangement creates a simple harmonic motion of the cylinder liner (5 and7). A mirror arrangement to the driven system (7) is used to in order to achieve dynamic balance. The ring holder (5) is instrumented with thermocouples and a piezoelectric load cell to measure the cylinder liner-ring contact friction. The test rig is heated through a heating block and a cartridge heater arrangement that encases the reciprocating liner throughout its stroke.

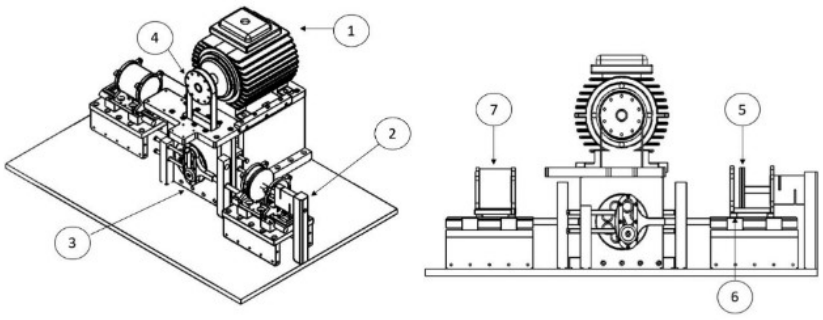

Figure 1: Test rig design. This figure is reproduced under the terms of the Creative Commons Attribution 4.0 License (https://creativecommons.org/licenses/by/4.0/) from original article by Forder et al [11]

The test rig is a 1:1 drive system which can operate in the speed range: 150-3000 rpm with the effective stroke length of 60 mm. The ring is loaded against the liner by tension of the segment and expander assembly. For these experiments a three=piece oil control ring produced by Nippon piston ring Corporation was used. The ring is made up of a 100 series (6227) steel with Titanium Nitride (TiN) running segmental faces. The two segments are separated by a waveform expander. The oil control ring is run against an 80 mm diameter bore cylinder liner made of a 19MNV6 stress relieved steel with Nickel Ceramic coating. The coated liner is cross-hatched with a 30° honing angle. The surface roughness properties of both the oil control ring and the cylinder liner are listed in Tables 1 and 2. The test lubricant is evenly applied via a graduated syringe to the liner surface at the beginning of each test.

Analytical Mixed-hydrodynamic lubrication model

An analytical model of an oil control ring-cylinder liner conjunction is made. It is assumed that the ring axial face-width profile is parabola. Therefore, the lubricant film profile can be described as:

$$h(x) = h_m + \frac{x^2}{2R} \tag{1}$$

where, h_m, x and R are the minimum film thickness, position along the ring face-width in the direction of sliding, and the radius of curvature of the ring profile respectively. The radial load is partially carried by hydrodynamics; W_h and partially by the interactions of surface asperities on the contiguous surface; W_a. Hence, the total contact load is:

$$W_t = W_h + W_a \tag{2}$$

Hydrodynamic load carrying capacity of the lubricant film is obtained based on a line contact hydrodynamics over a long rectangular footprint (if the ring is assumed as unwrapped) [12]:

$$W_h = \frac{2.45R\eta UL}{h_m} = \frac{2.45R\eta UL}{\lambda_m \sigma} \tag{3}$$

where, η, U, and L are the lubricant's dynamic viscosity, speed of entraining motion, and ring circumference length respectively. In the test rig described in the previous section the cylinder liner moves with a sinusoidal velocity profile. Thus, the speed of entraining motion becomes: $U = r\omega \cos \omega t$. Variables r and ω are the crank radius of the scotch yoke mechanism and the angular velocity of the crank. The minimum film thickness can be written in terms of the Stribeck parameter: $\lambda_m = h_m/\sigma$, where σ is the composite root mean square of asperity heights of the contacting surfaces.

The contact load is partially carried by the boundary interactions of the ring and the liner surface asperities in mixed regime of lubrication. The load carried by the asperities can be predicted using the Greenwood and Tripp [13] asperity contact model. Due to the curvature of the ring profile, the Greenwood and Tripp [13] model should be applied to a parabolic ring profile. The modified asperity load is predicted using the approach described by Gore et al [14]:

$$W_a = \frac{16\sqrt{2}}{15}\pi(\eta_a \beta_a \sigma)^2 \sqrt{\frac{\sigma}{\beta_a}} E^* L \sqrt{2R\sigma} \int_{\lambda_m}^{\lambda_c} F_{\frac{5}{2}}(\lambda)\, \lambda^{-1/2}\, \mathrm{d}\lambda \tag{4}$$

where, η_a and β_a are the asperity density per unit area of contact and the average radius of curvature of asperities tips respectively. E^* is the combined (reduced) Young's modulus of elasticity of the contacting surfaces: $\frac{1}{E^*} = \frac{1-\vartheta_1^2}{E_1} + \frac{1-\vartheta_2^2}{E_2}$ ($E_{1,2}$ and $\vartheta_{1,2}$ are the moduli of elasticity and Poisson's ratios of the contacting surfaces). The Stribeck parameter λ is variable along the width of contact, where a critical Stribeck parameter value $\lambda_c = \frac{h_c}{\sigma} = 4.0$ denotes fully flooded condition (no asperity interactions). An exponential function-fit, proposed by Dolatabadi et al [15], is used for the probability function $F_{5/2}$ defined by Greenwood and Tripp [13] as:

$$F_{\frac{5}{2}}(\lambda) = 6.879 \exp\left(-\frac{(\lambda+2.791)^2}{2\times 1.271^2}\right) \quad (5)$$

The real contact area is determined by Gore et al [14] as:

$$A_a = \pi^2(\eta_a \beta_a \sigma)^2 L\sqrt{2R\sigma} \int_{\lambda_m}^{\lambda_c} F_2(\lambda)\lambda^{-1/2} \mathrm{d}\lambda \quad (4)$$

where, $F_2(\lambda)$ is a second probability function based on the Greenwood and Tripp [13]. This function can be approximated by a fitted exponential function [16] as:

$$F_2(\lambda) = 3.585 \exp\left(-\frac{(\lambda+2.495)^2}{2\times 1.257^2}\right) \quad (5)$$

The total friction f_f of the oil control ring-liner contact is defined as:

$$f_f = f_{f,v} + f_{f,b} \quad (6)$$

where, the viscous friction is predicted using the analytical method in Rahmani and Rahnejat [17]:

$$f_{f,v} = -\frac{A_1+A_2+A_3}{4\zeta\sqrt{\zeta-1}} \eta U \left(\frac{2b}{h_m}\right) L \quad (7)$$

The ring face half-width is b. Coefficients A_i are provided in equation (8)

$$\begin{cases} A_1 = [(12\zeta^2 - 12\zeta)c^2 - 3\zeta]\,\mathrm{atan}\left(2c\sqrt{\zeta-1}\right) \\ A_2 = [(12\zeta^2 - 12\zeta)c^2 - 7\zeta]\,\mathrm{atan}\left(\sqrt{\zeta-1}\right) \\ A_3 = 12\left(c+\frac{1}{2}\right)\sqrt{\zeta-1}\left(\frac{1}{2} + (\zeta-1)c\right) \end{cases} \quad (8)$$

where, $c = 0.24636\,\zeta^{-0.5062}$ and $\zeta = h(x-b)/h_m$ is determined based on equation (1). Boundary friction depends on the Eyring limiting shear stress τ_0, real contact area of asperities A_a, pressure coefficient of boundary shear strength ξ and the asperity contact load W_a. Thus:

$$f_{f,b} = \tau_0 A_a + \xi W_a \quad (9)$$

Finally, the coefficient of friction is predicted by equation (10).

$$\mu = f_f / W_t \quad (10)$$

Results

The thermal and mechanical properties of the surfaces are provided in Table 1 for both the liner and the coated oil control ring. The surface topographical parameters for the piston rings [14] are shown in Table 2. A lubricant grade of 0W40 is used in the tribometer for the experimental measurements and the lubricant properties are provided in Table 3, for use in the numerical analysis. Simulations are run at two lubricant temperatures of 20 °C and 80 °C. The dynamic viscosity of lubricant is 101.3 and 15.2 mPa.s at these temperatures, respectively.

Table 1. Bore and oil ring mechanical properties (Dolatabadi et al. [14])

Parameter	Ring coating, TiN	Bore coating, Nickel ceramic	Unit
Young's modulus of Elasticity	251	165	GPa
Poisson ratio	0.25	0.31	--
Density	5220	5175	kg m^{-3}
Thermal conductivity	19.2	42.1	W m^{-1} K^{-1}
Specific heat capacity	484.9	566	J kg^{-1} K^{-1}
Coating thickness	1.5-3	50-70	μm

Table 2. Surface topography of the coated ring and bore

Parameter	Ring coating, TiN	Unit
Composite Root mean square height, σ	0.433±0.02	μm
Surface parameter ($\sigma\beta_a\eta_a$)	1.560	--
Surface parameter (σ/β_a)	1.200×10^{-4}	--
Pressure coefficient of boundary shear, ξ	0.26	--

Table 3. Oil specifications (0W40)

Parameter	Value	Unit
Density	855 @15 °C	kg.m^{-3}
Kinematic viscosity	67.61 @40 °C, 12.25 @ 100 °C	cSt
Thermal conductivity	0.255	W m^{-1} K^{-1}
Specific heat capacity	2360	J kg^{-1} K^{-1}
Thermal expansion coefficient	6.5×10^{-4}	K^{-1}
Pressure viscosity coefficient at atmospheric pressure	10	GPa^{-1}
Eyring shear stress limit	2	MPa

The assembled oil control ring tension force is measured using a ring tensioning device as 70 N. It is assumed that the tension force is equally distributed between the two ring segments circumferentially. Therefore, the applied contact force is 35 N on each segment. The measured ring friction is compared with the prediction at the two temperatures shown in figure 2(a) and 2(b). The measured values show that asperity contact between the contiguous surfaces is the main contributor to the overall friction. This effect is more dominant at 80 °C, where friction increases during reversals with reduced lubricant viscosity (thus more boundary interactions. Friction is more uniform throughout the stroke at 20 °C. Predicted friction results at 20 °C shows that the conditions are dominantly boundary at reversals, but at mid-span stroke, the contribution of boundary friction decreases, as the severity of mixed regime of lubrication is reduced. The difference in experimental and modelling results can be attributed to lubricant starvation in practice (not accounted for in the numerical analysis).

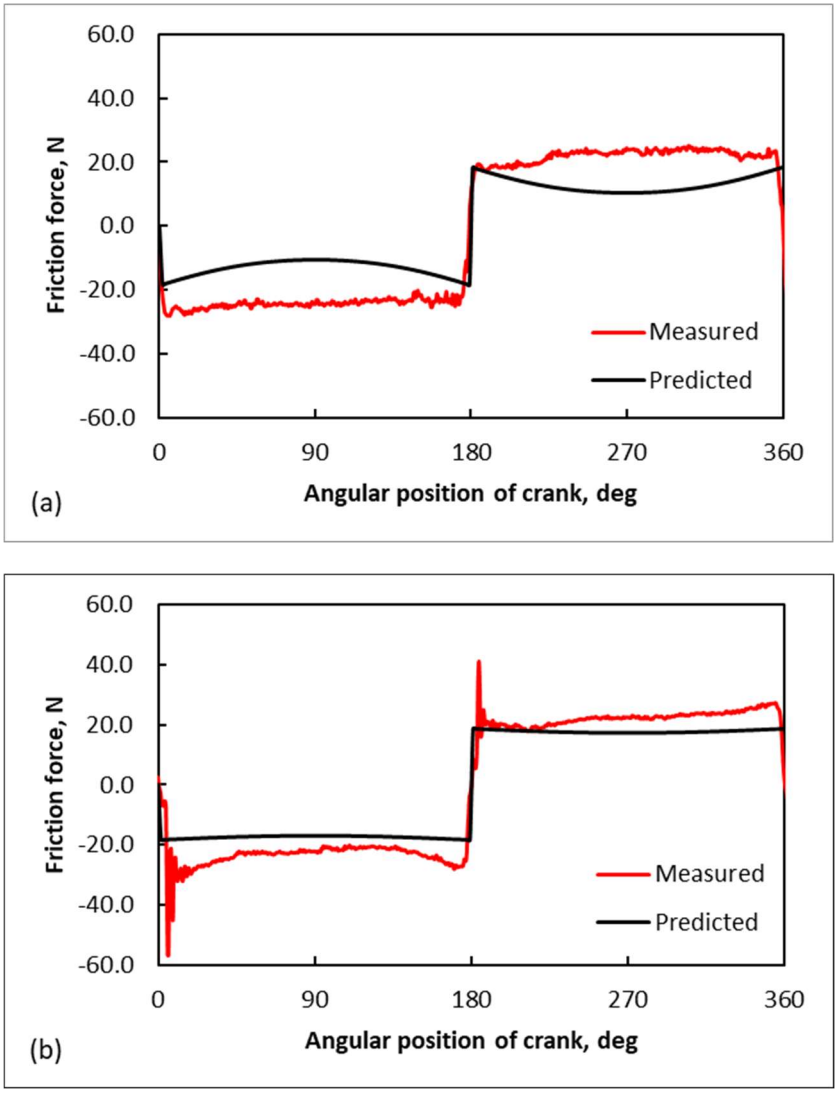

Figure 2: Comparison of predicted and measured friction forces of oil control ring for low viscosity engine oil at (a) 20 °C and (b) 80°C with crank speed of 300 rpm

At higher temperatures, the viscosity of the lubricant reduces (and also the hydrodynamic load carrying capacity) and the radial load is carried by the asperities even at the mid-stroke of the cycle. Noticeably the increased friction occurs just after the reversal rather than during the approach. This may in part be due to the squeeze film support (despite negligible viscosity, again not included in equation (3)), delaying full contact between the segment faces and liner during dead centre approach. In addition, Nautiyal, Singhal and Sharma [18] have shown that boundary friction coefficients increase at elevated temperatures for similar conjunctions. This explains the high momentary friction at the start of each stroke required to overcome stiction.

Conclusion

This paper presents a combined experimental and numerical modelling approach to improve understanding of three-piece oil control ring-cylinder liner friction. The measurements highlight that the segment-liner conjunction traverses boundary and mixed regimes of lubrication. At higher temperatures, asymmetry is observed in friction during dead centre approach and reversal is observed. The numerical modelling approach is capable of predicting the magnitude of friction and determining viscous and boundary frictional contributions.

References

[1] Profito, F.J., Tomanik E. and Zachariadis D.C., "Effect of cylinder liner wear on the mixed lubrication regime of TLOCRs", Tribology Int., 2016, 93: 723–732.

[2] Söderfjäll, M., Almqvist, A. and Larsson, R., "A model for twin land oil control rings". Tribology Int., 2016, 95: 475-482.

[3] Söderfjäll, M., Almqvist, A. and Larsson, R., "Component test for simulation of piston ring–cylinder liner friction at realistic speeds", Tribology Int., 2016, 104: 57-63.

[4] Liu, Y., Kim, D., Westerfield, Z., et al., "A comprehensive study of the effects of honing patterns on twin-land oil control rings friction using both a numerical model and a floating liner engine", Proc. IMechE Part J: J. Engineering Tribology, 2019; 233: 229–255.

[5] Westerfield, Z., Tian, T., Liu, Y. and Kim, D., "A study of the friction of oil control rings using the floating liner engine", SAE Int. J. Engines, 2016, 9(3): 1807-1824.

[6] Kikuhara, K., Koeser, P.S. and Tian, T., "Effects of a cylinder liner microstructure on lubrication condition of a twin-land oil control ring and a piston skirt of an internal combustion engine", Tribology Lett., 2022, 70: 1-15.

[7] Tian, T., Wong, V.W. and Heywood, J.B., "Modeling the dynamics and lubrication of three piece Oil control rings is internal combustion engines", SAE Trans., 1998: 1989–2006.

[8] Zhang, W., Ahling, S. and Tian, T., "Modeling the three piece Oil control ring dynamics and Oil transport in internal combustion engines", SAE Tech. Pap. No. 2021-01-0345, 2021.

[9] Li, M. and Tian, T., "Effect of blowby on the leakage of the three-piece oil control ring and subsequent oil transport in upper ring-pack regions in internal combustion engines", Lubricants, 2022, 10(10): 250.

[10] Mochizuki, K., Sasaki, R., Iijima, N. and Usui, M., "Prediction and Experimental Verification for Oil Transport Volume around Three-Piece Type Oil Control Ring Affecting Lubricating Oil Consumption", SAE Int. J. Advances and Current Practices in Mobility, 2022, 5(2022-01-0522): 595-609.

[11] Forder, M.D., Morris, N., King, P., Balakrishnan, S. and Howell-Smith, S., "An experimental investigation of low viscosity lubricants on three piece oil control rings cylinder liner friction", Proc. IMechE, Part J: J. Engineering Tribology, 2022, 236(11): 2261-2271.

[12] Gohar, R. and Rahnejat, H., "Fundamentals of Tribology", 3rd Edition, World Scientific, 2018

[13] Greenwood, J.A. and Tripp, J.H., "The contact of two nominally flat rough surfaces", Proc. IMechE, J. Mech. Eng. Sci., 1970,185(1): 625–633.

[14] Gore, M., Morris, N., Rahmani, R., Rahnejat, H., King, P.D. and Howell-Smith, S., "A combined analytical-experimental investigation of friction in cylinder liner inserts under mixed and boundary regimes of lubrication", Lubrication Science, 2017, 29(5): 293-316.

[15] Dolatabadi, N., Forder, M., Morris, N., Rahmani, R., Rahnejat, H. and Howell-Smith, S., "Influence of advanced cylinder coatings on vehicular fuel economy and emissions in piston compression ring conjunction", Applied Energy, 2020, 259, p.114129.

[16] Dolatabadi, N., Rahmani, R., Rahnejat, H., Garner, C.P. and Brunton, C., "Performance of poly alpha olefin nanolubricant", Lubricants, 2020, 8(2):17.

[17] Rahmani, R. and Rahnejat, H., "Enhanced performance of optimised partially textured load bearing surfaces", Tribology Int., 2018 117: 272-282.

[18] Nautiyal, P.C., Singhal, S. and Sharma, J.P., "Friction and wear processes in piston rings", Tribology Int., 1983, 16(1): 43-49.